Low Temperature Physics/Fizika Nizkikh Temperatur, 2020, v. 46, No. 2, pp. 121–129

Phase diagram of hydrogen at extreme pressures and temperatures; updated through 2019

(Review Article)

Alexander Goncharov

Geophysical Laboratory, Carnegie Institution of Washington
5251 Broad Branch Rd., NW, Washington, DC 20015, USA
E-mail: agoncharov@carnegiescience.edu

Received October 9, 2019, published online December 27, 2019

Hydrogen is expected to display remarkable properties under extreme pressures and temperatures stemming from its low mass and thus propensity to quantum phenomena. Exploring such phenomena remains very challenging even though there was a tremendous technical progress both in experimental and theoretical techniques since the last comprehensive review (McMahon *et al.*) was published in 2012. Raman and optical spectroscopy experiments including infrared have been extended to cover a broad range of pressures and temperatures (*P*–*T*) probing phase stability and optical properties at these conditions. Novel pulsed laser heating and toroidal diamond anvil techniques together with diamond anvil protecting layers drastically improved the capabilities of static compression methods. The electrical conductivity measurements have been also performed to much higher than previously pressures and extended to low temperatures. The dynamic compression techniques have been dramatically improved recently enabling ramp isentropic compression that allows probing a wide range of *P*–*T* thermodynamic pathways. In addition, new theoretical methods have been developed beyond a common DFT theory, which make them predictive and in better agreement with experiments. With the development of new theoretical and experimental tools and sample loading methods, the quest for metallic hydrogen accelerated recently delivering a wealth of new data, which are reviewed here.

Keywords: hydrogen, extreme pressures, solid phases of hydrogen, plasma transition, metallic hydrogen.

Contents

Introduction

Hydrogen is a fascinating material possessing the unique properties owing to its unique position as the element one in the Periodic Table. Since it is the most spread element in the Universe, the physical and chemical properties of hydrogen at extremes are of great interest for planetary science. It is also the most simple element, for which the quantum mechanics problems can be solved exactly [1]. Based on its position as the group one element it should be metal but because there are only two electrons in the first electronic shell, hydrogen is also a halogen forming a diatomic molecule at ambient conditions. Unlike other simple molecular material, quite a high pressure likely in excess of 5 Mbar (500 GPa) is needed to make a monoatomic configuration of hydrogen stable. No matter, how high this value occurs to us, this pressure is a small fraction of the atomic unit of pressure $E_h/a_0^3 = 2.9421912 \cdot 10^{13}$ Pa = 29.422 GPa = = 29.422 TPa = 294 Mbar, which corresponds to a substantial perturbation of the electronic atomic levels. These con-

siderations make the study of hydrogen at very high-pressure fundamental for our understanding of chemical bonding in materials. In this regard, the metallization of hydrogen and related to this possible superconductivity and superfluidity is of particular interest [2,3]. Initially predicted in a solid state by Wigner and Huntington in 1935 at 25 GPa [4], it remains the Holy Grail for the high-pressure studies until now. Although there is no doubt that hydrogen metallizes and eventually transforms into a monatomic metal at high pressure, the transformation pathway and the intermediate phases remain enigmatic for both theory and experiment. It is much clearer for metallization of fluid hydrogen, but the existing data are largely contradictory, justifying further investigations.

In this paper, I overview the research progress in investigations of hydrogen a very high pressures since the last comprehensive review [1]. Other more specialized review articles are devoted to diamond anvil cell (DAC) experiments [5] and public debates on metallic hydrogen at the AIRAPT-26 Meeting (2017) in Beijing [6]. I will start this review from recent technical developments enabling the research progress in experiment in theory, which described after.

Technical developments

Theory. Density functional theory (DFT) calculations, which become the major tool for the materials research now and are adequate in the vast majority of the cases including the structural predictions (e.g., Ref. 7), are insufficient for hydrogen at high pressure. This has been demonstrated both for determinations of the stable solid phase stability as well as in exploring extreme high pressure-temperature (P–T) conditions. For choosing the most stable crystal structures, one needs very accurate calculations with an energy resolution of a few meV per atom (e.g., Ref. 8). This level of accuracy for hydrogen structures cannot be provided by DFT as evidenced by calculations with different exchange correlation functions and because of disagreements with the experiments concerning the most stable structure, which results in incorrect description of metallization pressure [8]. The diffusion quantum Monte Carlo (QMC) method [9] is more accurate for such studies [10,11], which has been recently demonstrated for structural studies of hydrogen at high pressures (see below). Moreover, the small mass of H atom and weak interatomic bonding at high pressures results in the requirement of a full treatment of quantum nuclear vibrational motion, which was performed using a DFT-based vibrational self-consistent field approach [12] to calculate anharmonic vibrational energies, which are essential in evaluating the lattice energy and, thus, the structural stability.

Nuclear quantum fluctuations are also important for understanding of the phase diagram of hydrogen (Fig. 1) in the regime of orientational ordering, where strong isotope effects have been documented (see Ref. 13 and Refs. therein). By combining DFT with a path-integral molecular dynamics (PIMD) these quantum effects can be at least qualitatively understood [13–15].

Going beyond the classical DFT methods is also important for understanding the liquid-liquid transition in hydrogen, where newly developed coupled electron-ion Monte Carlo (CEIMC) simulations provide the most adequate description of the process of molecular dissociation [16,17].

Experiment. Technical challenges related to static compression of hydrogen are two-fold [5]. (i) Hydrogen is very compressible making it hard to squeeze employing incompressible materials of DAC, for example rhenium gasket. (ii) Hydrogen is highly diffusive and tends to penetrate and

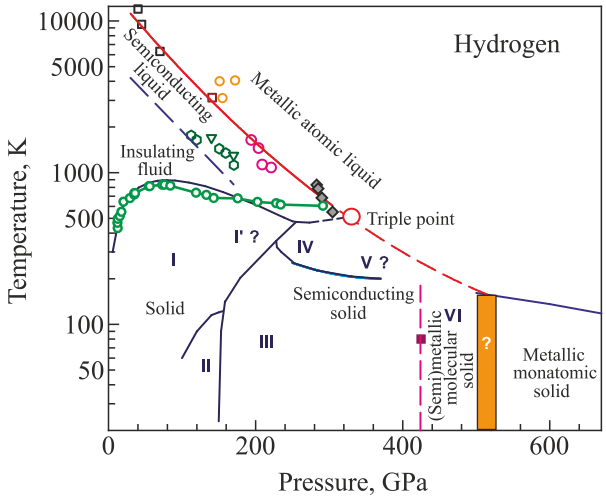

Fig. 1. (Color online) Phase diagram of hydrogen at high pressures and various temperatures. The solid dark blue lines are the phase lines between the solid molecular phases and the melt line from Refs. 33–35 and the dashed line is the extrapolation of the melt line to higher pressures. An alternative and substantially different set of measurements of the melt line by Zha *et al.* [36] is depicted by open green circles and solid green lines. A solid pink square corresponds to an IR bandgap closure reported by Loubeyre *et al.* [21]. A vertical dashed pink line is a proposed associated phase line between a semiconducting and semi(metallic) molecular phase also probed via the electrical conductivity by Eremets *et al.* [24]. A hypothetic transition to an atomic metallic phase is shown by an orange box. At higher pressure theory predicts an atomic metallic phase with a declining melt line shown by a solid blue line [37]. At high temperature, the experiments and theory show two almost parallel boundaries corresponding to a transition into a semiconducting state (dashed blue line) and insulator-metal transition (solid red line). These have been measured by direct and indirect DAC and dynamic compression techniques [38–45]. Green symbols correspond to the DAC reflectance measurements in a pulsed laser-heated DAC [46,47], which disagree with other DAC pulsed laser heating reflectance experiments shown by open orange circles [29]. Open black squares are from laser shocks [43], open pink circles are from laser-driven ramp compression [42], and grey diamonds are the Z-machine dynamic data [41], which were temperature corrected in Ref. 42.

react with the DAC materials causing premature breakage, especially at high temperatures. Since 2013 [5], the DAC technology has made another leap, at least partially overcoming the above-mentioned issues and thus enabling static experiments beyond 400 GPa.

Toroidal diamond anvils have been designed and realized in static experiments [18,19] yielding much higher pressures than can be normally achieved with the beveled DAC. The advantage of this geometry compared to previously reported double-stage anvils [20] is better compatibility with a variety of different samples including gas loaded such as hydrogen [21]. Recently pressures in excess of 425 GPa have been reached with hydrogen at 80 K [20,21]. While even higher pressures have been reported in experiments using conventional beveled anvils [23,24], the toroidal DAC appears to have an important advantage in the capability to perform experiments both on compression and decompression. Moreover, the true pressure reached in these ultrahigh-pressure experiments depends strongly on the pressure metrology, which remains challenging often producing inconsistent results [25–27].

A variety of methods has been used to reduce the probability of premature anvil failure due to hydrogen diffusion. It includes a combination of anvil fine polishing, annealing, and coating by various materials mainly Au (very thin layer) and alumina [23,28,29]. Use of pulsed laser heating techniques combined with spectroscopy (e.g. Ref. 30) enabled investigations of liquid states of hydrogen and other materials [29,31,32].

Phase transitions in solid molecular phases at low temperatures

At low to moderate pressures, molecular diatomic hydrogen has two major phases. Phase I is a plastic crystal-forming an hcp lattice of freely rotating H_2 molecules. At room temperature, this phase is stable up to 200 GPa. At low temperatures, where the rotations become hindered, the molecules tend to order forming phase II (known also as a broken symmetry phase), and pressure stabilizes the ordering as the anisotropic interactions increase with pressure. However, the *P*–*T* conditions of stability and even the phase symmetry strongly depend on the rotational state of the molecule described via the rotational molecular angular momentum J related to the molecular nuclear spin I_N through the symmetry considerations [48]. For hydrogen molecule with two protons with spin 1/2 each, there are two forms of H_2 molecule: parahydrogen (*p*) with antisymmetric nuclear spin functions and hence symmetric rotational wave functions, and vice versa for orthohydrogen (*o*). Orthohydrogen with elongated dumbbell-shaped molecules forms an orientationally ordered *Pa*3 structure at 0 GPa (where the dominated quadrupolar interactions are minimized), however the orientation ordering transition shifts too much higher pressures for spherical parahydrogen and the character of the ordering changes. For deuterium, the ortho-para nomenclature is the opposite for the molecular shapes as the nuclear spin is different (I_N = 1 vs 1/2 in H_2). Because of technical problems, the majority of high-pressure experiments on H_2 and D_2 are performed on the samples with a natural equilibrium or close to equilibrium concentration of ortho- and para-species, making the interpretation more difficult. The I–II phase lines for these close to normal (*n*) H_2 and D_2 are shifted to lower pressure compared to pure *p*-H_2 and *o*-D_2; the lattice symmetry is believed to be close to *hcp*, but the exact crystal structure is unknown. It is remarkable that HD molecules, where spin symmetry rules are relaxed and there is no *o*-*p* distinction, show an interesting reentrance behavior for phase II, where an orientationally ordered phase II transforms to a rotationally disordered phase I on cooling [49–51]. This can be qualitatively understood as due to the higher entropy of the broken symmetry phase of HD due to a equivalence of H and D.

Theoretical treatment of phase II is very complex, as it should include nuclear quantum motions and exchange contributions. The most recent DFT calculations [8,52,53] suggest $P6_3/m$ and $P2_1/c$-24 structures for phase II, with the latter one being slightly more stable and in a better agreement with the experimental Raman and IR spectra. QMC calculations and also an inclusion of anharmonic zero-point motion (ZP) support the stability of $P2_1/c$ structure [8]. However, the nuclear quantum fluctuations and *o*-*p* distinction are not a part of these theoretical calculations. In the most recent attempt to include the nuclear quantum motion, DFT treatment of` electrons was combined with a path integral molecular dynamics [13]. The results suggest a prediction of a clear distinction of phase II in H_2 and D_2, where D_2 forms an orientationally ordered structure, while H_2 remains a “quantum fluxional solid” [54] in the sense that the molecules remain very large asymmetric angular quantum fluctuations. This result is somewhat in odd with the previous similar calculations [14], where a quantum localization, which means in this case restrictions of rotations in certain directions, has been reported.

The experiments on phase II are very scarce concerning the structural information; neutron and x-ray diffraction (XRD) experiments suggest an additional incommensurate order in the *a* direction in D_2 [55], which is broadly consistent with additional Raman peaks observed in phase II of D_2 and interpreted as due to a superstructure [56]. Raman and IR spectroscopy remain the major tools in probing hydrogen at very high pressures. A recent Raman investigation claims the existence of a second phase II in D_2 based on a change with pressure in a character of an anomaly in the temperature dependence of the Raman intramolecular stretching mode (vibron) related to the II–I transition [57]. This has been noticed also in the previous measurements [33] and was interpreted as a change in sign in the vibron shift at the transition. The existence of the second phase II in D_2 was criticized [58] based on the data insufficiency to support the change in symmetry. The definitive answer to this dis-

cussion requires high-quality single-crystal XRD data, the technique, which has been enormously progressed recently for the DAC research (e.g., Ref. 59). Vibrational spectra of phase II of H_2 remain scarcely studied. As in D_2, the I–II transition in *n*- and *p*- H_2 is manifested by the appearance of additional low-frequency bands [56,57,60], interpreted as librons (lattice phonons derived from restricted rotational motion), which supplant the rotons (free molecular rotations) of phase I. However, the rotons (which split) and librons coexist in phase II of H_2 and D_2 [56,57,60]. This complex vibrational behavior still needs to be explained in future investigations.

Phase III of hydrogen (known also as H–A phase) is a high-pressure phase which occurs above approximately 160 GPa in both H_2 and D_2. Owing to the vibrational spectra, which are rich for the pressure-dependent libron modes and have no rotons, and nearly no isotope effect on the critical pressure, this phase has been understood as a classical orientationally ordered one, where the ordering objects are the molecules themselves [61]. This justifies the use of DFT as the first approximation in the structural search for phase III, where XRD data remain very limited and insufficient for the complete structural determination [62,63]. Pickard and Needs [52] found that a monoclinic structure *C*2/*c*-24 provides a good match to the experimental vibrational data for phase III and is the lowest-enthalpy phase over the pressure range, where phase III is observed (160–300 GPa). However, the calculated XRD of *C*2/*c* H_2 is largely inconsistent with the observations that show that phase III has a lattice of molecular centers, which is close to *hcp* [62,63]. In a more recent DFT calculations, where the effects of nuclear quantum and thermal vibrations are incorporated, it has been found that another (hexagonal) and also layered $P6_122$-36 structure is more stable than *C*2/*c* below about 200 GPa. XRD of $P6_122$ structure is more consistent with *hcp* lattice [64]. The *C*2/*c* and $P6_122$ structures are similar in molecular stacking but $P6_122$ has a larger number of layers in the unit cell. Recent Raman investigation beyond 300 GPa [62] reported a change in slope and splitting of the low-frequency librons, interpreted as a structural phase transition. These results are not inconsistent with the previously published Raman and IR data [65–67], where no phase transition was reported in this pressure range. Moreover, the stability of phase III up to higher pressures of 360 GPa [67], 440 GPa [24], 425 GPa [21] has been reported. A new low-temperature phase evidenced via an abrupt change in the IR vibron spectra (a signature band of phase III) at 356 GPa [68] has not been confirmed by other studies. A major change in electrical conductivity and optical properties have been reported at 360 GPa [24] and 425 GPa [21] as will be described below.

Phase transitions in solid phases at room temperature

Phase IV of hydrogen encounter at room temperature above 220 GPa [28,69] was a surprise, as DFT theory did not predict the stability of the hydrogen phase with such a great distinction in the vibron frequencies. A *Pbcn* structure with the molecular arrangement, where there are molecular layers of two kinds: weakly bound hexagonal, and strongly bound graphene-like was predicted by Pickard and Needs [52], but it was found metastable. Instead, DFT theory predicts the stability of a metallic *Cmca*-12 and *Cmca*-4 with a single kind of molecules. However, QMC theory [8,70] reranks the phase stability promoting semiconducting *C*2/*c*-24 (phase III) and *Pc*-48 (phase IV). As we mentioned above, $P6_122$ structure was found slightly more stable than *C*2/*c* below 200 GPa [64].

Phase IV with a very unusual molecular structure (coined as a mixed molecular and atomic [69]) was a focus of many experimental and theoretical investigations aiming to understand better the structure and dynamics of this phase that was thought to be a precursor of molecular dissociation. Indeed, there are a number of interesting phenomena observed in phase IV under pressure. The Raman vibron in the graphene layers dramatically softens and broadens suggesting the approaching molecular instability [69,71]. A reduced isotope effect evidence for significant anharmonic and quantum effects, which increase with pressure [71]. The absorption edge is quite broad and it is redshifted with pressure [69,71,72]. Molecular dynamics calculations [71,73–75] have been used to understand the nature of the quantum effects and possible diffusive motion of the atoms. The results of different investigations are somewhat contradictory, however a large proton motion has been confirmed that show that the structure of phase IV is highly dynamic. The atoms in the elongated molecules of the graphene-like layer show a diffusive motion, which can be viewed as the rotation of a three-molecule ring and an even long-range atomic migration. This can cause a change in the chemical bonds location, which migrate with time, yet preserving the local lattice symmetry at each time. These unusual lattice dynamics must result in modified structural and vibrational characteristics that are different from an ideal diffusionless structure [74]. The number of the observed Raman and IR modes is much less than predicted for the best theoretical *Pc*-48 structure [70,76], which can be tentatively explained by the peak broadening and merging with the stronger bands. Intermolecular coupling is greatly modified in phase IV compared to phases I and III and becomes highly heterogeneous between weekly and strongly bound molecular layers. It is much stronger in the graphene-like layer and continues to increase with pressure as it has been deduced from simultaneous Raman and IR measurements [22] (cf. Ref. 77).

A number of Raman, IR, and optical spectroscopy experiments at room temperature have been reported to higher pressures up to 388 GPa [78,79] that show that the spectra of phase IV evolve under pressure suggesting that some additional structural transformations might occur. Phase IV′ was proposed to appear above 275 GPa in H_2 based on a change in pressure slope of the Raman vibron frequency in

the graphene layer ν_1 and the bandgap, and other minor spectral changes [72]. However, these changes are too subtle to signify significant structural changes. Zha *et al.* reported a splitting of the main Raman vibron and some other minor changes in Raman intensity of the low-frequency modes [79], which again cannot be a definitive proof of a proposed structural transition (to phase V). In a subsequent Raman investigation [78], a structural transition to phase V was claimed at 325 GPa in H_2 based on a number of spectral changes that include disappearance of the low-frequency libron modes (L_2 and L_3), change in slope of the main Raman vibron, and a broadening of the lowest-frequency weakly pressure-dependent mode L_1. The behavior of the latter one corresponding to a collective rotation of a ring of three weakly bound H_2 molecules in the graphene-like layer [71,76] is of special interest. This mode and the vibron ν_1 are the signature modes of phase IV that clearly manifest the existence of weakly bound molecules even though they can be extremely short-lived. Their disappearance would signal molecular dissociation for example into the *Ibam* structure, in which the weakly bound layer is truly graphene-like with all equal interatomic distances. Phase IV can be considered as the dynamically Peierls-distorted [80] *Ibam* structure. Remarkably, *Ibam* structure is dynamically unstable in harmonic approximation but stabilizes via anharmonic vibrations and it is energetically competitive [70]. Reported in Refs. 78,79, decrease in intensity of the Raman libron modes and change in the pressure slope of the ν_1 mode do not signify a structural transition nor molecular dissociation of phase IV. Indeed, the Raman frequencies and intensities can be renormalized due to the mode coupling of the same symmetry. In this regard, one should note that the Raman intensities and their change depend on the proximity in energy of the coupled modes, which changes under pressure due to strong pressure dependencies of the frequencies of some modes (e.g., ν_1). Some of the observations of the intensity redistributions of the libron modes under pressure [72,78] can be explained by the pressure-dependent mode coupling [71], while other observations (e.g., ν_1 and L_1 line broadening) may stem from the tendency of the phase IV to transform to the *Ibam* structure, where one expects much less Raman activity and strongly damped optical phonons. The most recent theoretical investigations including QMC calculations suggested another mixed layered monoclinic $Pca2_1$ structure as a possible phase V, however, the arguments for its existence and matching with the experiment are not definitive [70].

XRD could be thought to immediately address the structural uncertainties described above concerning phases II, III, and IV. However, the most direct XRD technique can only detect the averaged overtime structure. Thus, the results for highly dynamic but yet quantum or locally ordered phases II and IV [50,62,63] should be considered with caution. Moreover, the available XRD data do not represent the results of a full single-crystal collection and analysis, and instead determine only the *d*-spacings [81]. Thus, the Raman and IR spectroscopy methods, which probe the chemical bonds and local order directly, remain crucial for exploring hydrogen at high pressures [22].

Whether hydrogen in phase IV (or V) transforms to a molecular (e.g., *Cmca*-4), mixed (e.g., *Ibam*), or monatomic (e.g., $I4_1/amd$ [10,11]) solid or even liquid [37] at room temperature on the further compression at room temperature remains uncertain. While molecular or mixed solid phases are the most plausible candidates for the solid [37] and are likely metallic, the liquid monatomic liquid is definitely metallic. The melting curve of hydrogen has been shown to turn over at about 80 GPa, and it stays below 700 K above 200 GPa (Fig. 1) [34,36]; no DAC experiments on melting have been reported above 300 GPa. The DAC experiments in this regime might be quite challenging for the years to come, while dynamic ramp compression experiments using either electromagnetic (*Z*-machine) or laser-driven compression can probe *P*–*T* range slightly above room temperature and pressures in access of 300 GPa [41,42]. The latter experiments showed an abrupt change in the optical properties above 300 GPa [41] and 200 GPa [42], interpreted as the insulator to metal transition. The reason of such a disparity in pressure is likely due to different temperature conditions in these experiments; the temperate was not measured but rather inferred from the theoretical equation of state. Celliers *et al.* [42] suggested that temperatures were overestimated in the experiments of Knudson *et al.* [41], making the results of these experiments to match better; however, this temperature correction was debated [82,83]. In this regime, the plasma transition line is expected to be very close to the declining with pressure melting line [34,36,84] (Fig. 1). These lines should merge in a triple point, above which solid expected to melt into metallic liquid. At these conditions, only theory could currently be used to assess melting. Chen *et al.* [37] explored this regime in their PIMD calculations and found a further decline of the melting line suggesting that liquid hydrogen can be the ground state above 900 GPa. However, Geng *et al.* [85] found yet another solid atomic phase giving rise to the increased melting line above 2 TPa. Moreover, the calculations show the existence of a novel supersolid state at 1–1.5 TPa at elevated temperatures, where protons show a largely increased diffusivity while preserving the positioning order [15].

Insulator to metal transition in solid

Recently there were several experimental reports about accessing the metallic states of hydrogen in DAC at low temperatures (< 100 K) [21,23,24]. These experiments are very challenging in reaching the pressure range needed and probing the material at these conditions. Dias and Silvera [23] reported the optical reflectance of hydrogen at 495 GPa using four laser wavelengths in the spectral range of 0.75 and 3.1 eV. However, these experiments lack credi-

bility in many aspects including continuity of the results with those at lower pressure, pressure metrology, lack of the sample presence test in the DAC, lack of the energy loss calibration through the diamond anvils, inconsistency between the sample visual observations and the reflectance spectra with the documented previously diamond absorption among other less important [6,25,26,86,87]. Overall, Dias and Silvera's paper provides no valuable information about hydrogen metallization and no reliable characterization of the metallic phase [23]. Instead, Eremets *et al.* [24], and Loubeyre *et al.* [21] present useful and reliable data on the electrical and optical conductivity of hydrogen up to 480 GPa, which show that phase III of hydrogen experiences a bandgap narrowing and a possible closure. Optical probing below 0.1 eV would be required to understand possible interactions between the valence and conduction bands [88,89]. The optical [21] and electrical conductivity [24] experiments can be likely reconciled assuming that hydrogen experiences indirect bandgap closure above 400 GPa, which is broadly consistent with the theoretical calculations [90].

Insulator to metal transition in liquid

Concomitantly to the loss of molecular character and metallization of hydrogen in the solid-state one would expect a substantial change in the chemical bonding in the liquid state, which could be manifested as an abrupt liquid–liquid transition as in the case of phosphorous, for example [91]. The evolution of properties of the liquid with pressure represents a central question in the phase diagram of hydrogen where an atomic liquid metallic hydrogen is even expected to be a ground state at very high pressure (see above). The liquid–liquid phase transition in fluid hydrogen was predicted theoretically below a certain critical temperature [92–94], but the location of the critical point and the phase line varied depending on the level and type of calculations [95–99]. The CEIMC calculations [16] suggest that the dissociation and metallization transitions coincide (c.f. Ref. 100), and the critical point is located near 80–170 GPa and 1600–3000 K.

Dynamic compression experiments, which explore a variety of *P–T* pathways, agree on the existence of the metallic states detected via electrical, optical, and density measurements [41–45,101], while there are inconsistencies at low temperatures [41,42]. DAC experiments combined with laser heating probing relatively low-temperature fluid states have also yielded controversial results on the electronic properties of hydrogen and the location of the phase lines [32,38–40,46,47]. The difficulty of interpreting these optical DAC experiments is due to indirect probing of the state of hydrogen [38,39], or detection of reflectance signals superimposed with those of other materials in the DAC cavity and interpreted assuming *a-priori* a direct transformation from insulator to metal [32,46,47]. The latter results, reporting transient reflectance and transmission at a few laser wavelengths, have been found inconsistent with the proposed IMT, while an indirect transformation via intermediate-conductivity states is a plausible alternative [17,40–42,44,102]. One of the major drawbacks of the majority of preceding dynamic and static experiments is an extreme paucity of robust spectroscopic observations, which are critical for assessing the material electronic properties. Recently, Jiang *et al.* [29] reported the reflectance increasing rapidly with decreasing photon energy indicating free-electron metallic behavior with a plasma edge in the visible spectral range at high temperatures. They find the *P–T* conditions of the IMT close to those reported in shock wave experiments. The reflectance spectra suggest much longer electronic collision time (≥ 1 fs) than previously inferred, implying that metallic hydrogen at the conditions studied is not in the regime of saturated conductivity (Mott-Ioffe-Regel limit). The emerging phase diagram (Fig. 1) suggests the existence of a semiconducting intermediate fluid hydrogen state.

Conclusions and outlook

In this brief review, we showed that studies of hydrogen at extreme conditions have been rapidly progressed in the recent five years or so. New theoretical methods have been developed beyond a common DFT theory, which makes the theoretical calculations much more predictive and in a better agreement with the experiments. Both dynamic and static experiments have been developed to overcome previously experienced challenges. Dynamic ramp compression experiments can now probe much lower (compared to shock compression) temperature conditions reaching *P–T* conditions of static DAC experiments. DAC experiments on hydrogen have been extended to previously unattainable *P–T* conditions: almost up to 500 GPa and up to 4000 K. As the result of combined theoretical and experimental investigations, a new phase diagram of hydrogen emerges making a good guidance for future investigations of the predicted magnificent properties.

1. J.M. McMahon, M.A. Morales, C. Pierleoni, and D.M. Ceperley, *Rev. Mod. Phys.* **84**, 1607 (2012).
2. N.W. Ashcroft, *Phys. Rev. Lett.* **92**, 187002 (2004).
3. E. Babaev, A. Sudbø, and N.W. Ashcroft, *Nature* **431**, 666 (2004).
4. E. Wigner and H.B. Huntington, *J. Chem. Phys.* **3**, 764 (1935).
5. A.F. Goncharov, R.T. Howie, and E. Gregoryanz, *Fiz. Nizk. Temp.* **39**, 523 (2013) [*Low Temp. Phys.* **39**, 402 (2013)].
6. H.Y. Geng, *Matter and Radiation at Extremes* **2**, 275 (2017).
7. C.J. Pickard and R.J. Needs, *J. Phys.: Condens. Matter* **23**, 053201 (2011).
8. N.D. Drummond, B. Monserrat, J.H. Lloyd-Williams, P. López Ríos, C.J. Pickard, and R.J. Needs, *Nature Commun.* **6**, 7794 (2015).
9. W.M.C. Foulkes, L. Mitas, R.J. Needs, and G. Rajagopal, *Rev. Mod. Phys.* **73**, 33 (2001).

10. S. Azadi, B. Monserrat, W.M.C. Foulkes, and R.J. Needs, *Phys. Rev. Lett.* **112**, 165501 (2014).
11. J. McMinis, R.C. Clay, D. Lee, and M.A. Morales, *Phys. Rev. Lett.* **114**, 105305 (2015).
12. B. Monserrat, N.D. Drummond, and R.J. Needs, *Phys. Rev. B* **87**, 144302 (2013).
13. G. Geneste, M. Torrent, F. Bottin, and P. Loubeyre, *Phys. Rev. Lett.* **109**, 155303 (2012).
14. H. Kitamura, S. Tsuneyuki, T. Ogitsu, and T. Miyake, *Nature* **404**, 259 (2000).
15. H.Y. Geng, Q. Wu, and Y. Sun, *J. Phys. Chem. Lett.* **8**, 223 (2017).
16. C. Pierleoni, M.A. Morales, G. Rillo, M. Holzmann, and D.M. Ceperley, *Proc. Natl. Acad. Sci.* **113**, 4953 (2016).
17. G. Rillo, M.A. Morales, D.M. Ceperley, and C. Pierleoni, *Proc. Natl. Acad. Sci.* **116**, 9770 (2019).
18. A. Dewaele, P. Loubeyre, F. Occelli, O. Marie, and M. Mezouar, *Nature Commun.* **9**, 2913 (2018).
19. Z. Jenei, E.F. O'Bannon, S.T. Weir, and H. Cynn, *Nature Commun.* **9**, 3563 (2018).
20. N. Dubrovinskaia, L. Dubrovinsky, N.A. Solopova, A. Abakumov, S. Turner, M. Hanfland, E. Bykova, M. Bykov, C. Prescher, V.B. Prakapenka, S. Petitgirard, I. Chuvashova, B. Gasharova, Y.-L. Mathis, P. Ershov, I. Snigireva, and A. Snigirev, *Sci. Adv.* **2**, e1600341 (2016).
21. P. Loubeyre, F. Occelli, and P. Dumas, *arXiv:1906.05634* (2019).
22. A.F. Goncharov, I. Chuvashova, C. Ji, and H.-k. Mao, *PNAS* (2019).
23. R.P. Dias and I.F. Silvera, *Science* **355**, 715 (2017).
24. M.I. Eremets, A.P. Drozdov, P.P. Kong, and H. Wang, *Nature Phys.* 1246 (2019).
25. P. Loubeyre, F. Occelli, and P. Dumas, *arXiv:1702.07192v1* (2017).
26. X.-D. Liu, P. Dalladay-Simpson, R.T. Howie, B. Li, and E. Gregoryanz, *Science* **357**, eaan2286 (2017).
27. R.T. Howie, E. Gregoryanz, and A.F. Goncharov, *J. Appl. Phys.* **114**, 073505 (2013).
28. M.I. Eremets, and I.A. Troyan, *Nat. Mater.* **10**, 927 (2011).
29. S. Jiang, N. Holtgrewe, Z.M. Geballe, S.S. Lobanov, M.F. Mahmood, R.S. McWilliams, and A.F. Goncharov, *Adv. Sci.*, 190168 (2019).
30. R.S. McWilliams, D.A. Dalton, Z. Konôpková, M.F. Mahmood, and A.F. Goncharov, *Proc. Natl. Acad. Sci.* **112**, 7925 (2015).
31. S. Jiang, N. Holtgrewe, S.S. Lobanov, F. Su, M.F. Mahmood, R.S. McWilliams, and A.F. Goncharov, *Nature Commun.* **9**, 2624 (2018).
32. M. Zaghoo, R.J. Husband, and I.F. Silvera, *Phys. Rev. B* **98**, 104102 (2018).
33. A.F. Goncharov, R.J. Hemley, and H.-k. Mao, *J. Chem. Phys.* **134**, 174501 (2011).
34. R.T. Howie, P. Dalladay-Simpson, and E. Gregoryanz, *Nat. Mater.* **14**, 495 (2015).
35. M.I. Eremets, I.A. Troyan, and A.P. Drozdov, *arXiv:1601.04479v1* (2016).
36. C.-s. Zha, H. Liu, J.S. Tse, and R.J. Hemley, *Phys. Rev. Lett.* **119**, 075302 (2017).
37. J. Chen, Xin-Zheng Li, Qianfan Zhang, Matthew I.J. Probert, Chris J. Pickard, Richard J. Needs, Angelos Michaelides, and Enge Wang, *Nature Commun.* **4**, 2064 (2013).
38. V. Dzyabura, M. Zaghoo, and I.F. Silvera, *Proc. Natl. Acad. Sci.* **110**, 8040 (2013).
39. Kenji Ohta, Kota Ichimaru, Mari Einaga, Sho Kawaguchi, Katsuya Shimizu, Takahiro Matsuoka, Naohisa Hirao, and Yasuo Ohishi, *Sci. Rep.* **5**, 16560 (2015).
40. R.S. McWilliams, D.A. Dalton, M.F. Mahmood, and A.F. Goncharov, *Phys. Rev. Lett.* **116**, 255501 (2016).
41. M.D. Knudson, M.P. Desjarlais, A. Becker, R.W. Lemke, K.R. Cochrane, M.E. Savage, D.E. Bliss, T.R. Mattsson, and R. Redmer, *Science* **348**, 1455 (2015).
42. P.M. Celliers, M. Millot, S. Brygoo, R.S. McWilliams, D.E. Fratanduono, J.R. Rygg, A.F. Goncharov, P. Loubeyre, J.H. Eggert, J.L. Peterson, N.B. Meezan, S.L. Pape, G.W. Collins, R. Jeanloz, and R.J. Hemley, *Science* **361**, 677 (2018).
43. P. Loubeyre, S. Brygoo, J. Eggert, P.M. Celliers, D.K. Spaulding, J.R. Rygg, T.R. Boehly, G.W. Collins, and R. Jeanloz, *Phys. Rev. B* **86**, 144115 (2012).
44. S.T. Weir, A.C. Mitchell, and W.J. Nellis, *Phys. Rev. Lett.* **76**, 1860 (1996).
45. V.E. Fortov, R.I. Ilkaev, V.A. Arinin, V.V. Burtzev, V.A. Golubev, I.L. Iosilevskiy, V.V. Khrustalev, A.L. Mikhailov, M.A. Mochalov, V.Ya. Ternovoi, and M.V. Zhernokletov, *Phys. Rev. Lett.* **99**, 185001 (2007).
46. M. Zaghoo, A. Salamat, and I.F. Silvera, *Phys. Rev. B* **93**, 155128 (2016).
47. M. Zaghoo and I.F. Silvera, *Proc. Natl. Acad. Sci.* **114**, 11873 (2017).
48. I.F. Silvera, *Rev. Mod. Phys.* **52**, 393 (1980).
49. F. Moshary, N.H. Chen, and I.F. Silvera, *Phys. Rev. Lett.* **71**, 3814 (1993).
50. Y. Crespo, A. Laio, G.E. Santoro, and E. Tosatti, *Phys. Rev. B* **84**, 144119 (2011).
51. Yu.A. Freiman, S.M. Tretyak, A. Jezowski, and R.J. Hemley, *J. Low Temp. Phys.* **113**, 723 (1998).
52. C.J. Pickard and R.J. Needs, *Nat. Phys.* **3**, 473 (2007).
53. C.J. Pickard and R.J. Needs, *Phys. Status Solidi B* **246**, 536 (2009).
54. S. Biermann, D. Hohl, and D. Marx, *Solid State Commun.* **108**, 337 (1998).
55. I. Goncharenko and P. Loubeyre, *Nature* **435**, 1206 (2005).
56. A.F. Goncharov, J.H. Eggert, I.I. Mazin, R.J. Hemley, and H.-k. Mao, *Phys. Rev. B* **54**, R15590 (1996).
57. X.-D. Liu, R.T. Howie, H.-C. Zhang, X.-J. Chen, and E. Gregoryanz, *Phys. Rev. Lett.* **119**, 065301 (2017).
58. A.F. Goncharov and Y.A. Freiman, Comment, *Phys. Rev. Lett.* **122**, 199601 (2019).
59. I. Chuvashova, E. Bykova, M. Bykov, V. Svitlyk, B. Gasharova, Y.-L. Mathis, R. Caracas, L. Dubrovinsky, and N. Dubrovinskaia, *J. Solid State Chem.* **245**, 50 (2017).
60. A.F. Goncharov, R.J. Hemley, H.-k. Mao, and J. Shu, *Phys. Rev. Lett.* **80**, 101 (1998).

61. I.I. Mazin, R.J. Hemley, A.F. Goncharov, M. Hanfland, and H.-k. Mao, *Phys. Rev. Lett.* **78**, 1066 (1997).
62. Y. Akahama, Y. Mizuki, S. Nakano, N. Hirao, and Y. Ohishi, *J. Phys.: Confer. Ser.* **950**, 042060 (2017).
63. C. Ji, B. Li, W. Liu , J.S. Smith, A. Majumdar, W. Luo, R. Ahuja, J. Shu, J. Wang, S. Sinogeikin, Y. Meng, V.B. Prakapenka, E. Greenberg, R. Xu, X. Huang, W. Yang, G. Shen, W.L. Mao, and H.K. Mao, *Nature* **573**, 558 (2019).
64. B. Monserrat, R.J. Needs, E. Gregoryanz, and C.J. Pickard, *Phys. Rev. B* **94**, 134101 (2016).
65. A.F. Goncharov, E. Gregoryanz, R.J. Hemley, and H.-k. Mao, *Proc. Natl. Acad. Sci.* **98**, 14234 (2001).
66. P. Loubeyre, F. Occelli, and R. LeToullec, *Nature* **416**, 613 (2002).
67. C.-S. Zha, Z. Liu, and R.J. Hemley, *Phys. Rev. Lett.* **108**, 146402 (2012).
68. R. Dias, O. Noked, and I.F. Silvera, *arXiv:1603.02162v2* (2016).
69. R.T. Howie, C.L. Guillaume, T. Scheler, A.F. Goncharov, and E. Gregoryanz, *Phys. Rev. Lett.* **108**, 125501 (2012).
70. B. Monserrat, N.D. Drummond, P. Dalladay-Simpson, R.T. Howie, P. López Ríos, E. Gregoryanz, C.J. Pickard, and R.J. Needs, *Phys. Rev. Lett.* **120**, 255701 (2018).
71. A.F. Goncharov, J.S. Tse, Hui Wang, Jianjun Yang, V.V. Struzhkin, R.T. Howie, and E. Gregoryanz, *Phys. Rev. B* **87**, 024101 (2013).
72. R.T. Howie, T. Scheler, C.L. Guillaume, and E. Gregoryanz, *Phys. Rev. B* **86**, 214104 (2012).
73. H. Liu and Y. Ma, *Phys. Rev. Lett.* **110**, 025903 (2013).
74. I.B. Magdău and G.J. Ackland, *Phys. Rev. B* **87**, 174110 (2013).
75. H. Liu, J. Tse, and Y. Ma, *J. Phys. Chem. C* **118**, 11902 (2014).
76. C.J. Pickard, M. Martinez-Canales, and R.J. Needs, *Phys. Rev. B* **85**, 214114 (2012).
77. C.-s. Zha, Z. Liu, M. Ahart, R. Boehler, and R.J. Hemley, *Phys. Rev. Lett.* **110**, 217402 (2013).
78. P. Dalladay-Simpson, R.T. Howie, and E. Gregoryanz, *Nature* **529**, 63 (2016).
79. C.-s. Zha, R.E. Cohen, H.-k. Mao, and R.J. Hemley, *Proc. Natl. Acad. Sci.* **111**, 4792 (2014).
80. O. Dubay, G. Kresse, and H. Kuzmany, *Phys. Rev. Lett.* **88**, 235506 (2002).
81. L. Dubrovinsky, N. Dubrovinskaia, and M.I. Katsnelson, *arXiv:1910.10772v1* (2019).
82. M.P. Desjarlais, M.D. Knudson, and R. Redmer, *Science* **363**, eaaw0969 (2019).
83. P.M. Celliers, M. Millot, S. Brygoo, R.S. McWilliams, D.E. Fratanduono, J.R. Rygg, A.F. Goncharov, P. Loubeyre, J.H. Eggert, J.L. Peterson, N.B. Meezan, S. Le Pape, G.W. Collins, R. Jeanloz, and R.J. Hemley, *Science* **363**, eaaw1970 (2019).
84. S.A. Bonev, E. Schwegler, T. Ogitsu, and G. Galli, *Nature* **431**, 669 (2004).
85. H.Y. Geng and Q. Wu, *Sci. Rep.* **6**, 36745 (2016).
86. A.F. Goncharov and V.V. Struzhkin, *Science* **357**, eaam9736 (2017).
87. M.I. Eremets and A.P. Drozdov, *arXiv:1702.05125v1* (2017).
88. I.I. Naumov and R.J. Hemley, *Phys. Rev. Lett.* **117**, 206403 (2016).
89. I.I. Naumov, R.E. Cohen, and R.J. Hemley, *Phys. Rev. B* **88**, 045125 (2013).
90. W.L. Yim, H. Shi, Y. Liang, R.J. Hemley, and J.S. Tse, in: *Correlations in Condensed Matter under Extreme Conditions.*, A. La Magna and G. Angilella (eds.), Springer, Cham (2017).
91. Yoshinori Katayama, Takeshi Mizutani, Wataru Utsumi, Osamu Shimomura, and Masaaki Yamakata, *Nature* **403**, 170 (2000).
92. W. Ebeling and W. Richert, *Phys. Lett. A* **108**, 80 (1985).
93. D. Saumon and G. Chabrier, *Phys. Rev. Lett.* **62**, 2397 (1989).
94. W.R. Magro, D.M. Ceperley, C. Pierleoni, and B. Bernu, *Phys. Rev. Lett.* **76**, 1240 (1996).
95. W. Lorenzen, B. Holst, and R. Redmer, *Phys. Rev. B* **82**, 195107 (2010).
96. I. Tamblyn and S.A. Bonev, *Phys. Rev. Lett.* **104**, 065702 (2010).
97. M.A. Morales, C. Pierleoni, E. Schwegler, and D.M. Ceperley, *Proc. Natl. Acad. Sci.* **107**, 12799 (2010).
98. S. Scandolo, *Proc. Nat. Acad. Sci.* **100**, 3051 (2003).
99. M.A. Morales, J.M. McMahon, C. Pierleoni, and D.M. Ceperley, *Phys. Rev. Lett.* **110**, 065702 (2013).
100. G. Mazzola and S. Sorella, *Phys. Rev. Lett.* **114**, 105701 (2015).
101. P.M. Celliers, G.W. Collins, L.B. Da Silva, D.M. Gold, R. Cauble, R.J. Wallace, M.E. Foord, and B.A. Hammel, *Phys. Rev. Lett.* **84**, 5564 (2000).
102. A.F. Goncharov and Z.M. Geballe, Comment, *Phys. Rev. B* **96**, 157101 (2017).

Фазова діаграма водню при екстремальних значеннях тиску та температури; новітні дані 2019 р.

О. Гончаров

Очікується, що водень проявляє дуже цікаві властивості при екстремальних значеннях тиску та температури, які обумовлені його низькою масою та, внаслідок цього, схильністю до квантових ефектів. Вивчення таких явищ залишається дуже складною задачею, не зважаючи на величезний технічний прогрес, досягнутий як в експериментальних, так і в теоретичних методах, з моменту публікації останнього всебічного огляду (McMahon *et al.*) у 2012 році. Експерименти з комбінаційної та оптичної спектроскопії, які включають інфрачервону, було розширено, щоб охопити широкий діапазон значень тиску та температури. Нові методи імпульсного лазерного нагріву та тороїдальної алмазної наковальні разом із захисними шарами значно покращили можливості статичного стиску. Було також проведено вимірювання електропровідності при набагато більших значеннях тиску, ніж попередні, та поширено на низькі температури. Крім того, методи динамічного стиску були значно покращені, більше орієнтовані на ізоент-

ропійне стиснення, що дало можливість дослідити широкий спектр термодинамічних станів *P*–*T*. Останнім часом з розвитком нових експериментальних інструментів та методів завантаження зразків прискорився пошук металічного водню, що дозволило отримати безліч розглянутих у цій роботі нових даних.

Ключові слова: водень, екстремально високі значення тиску, тверда фаза водню, плазменний перехід, металічний водень.

Фазовая диаграмма водорода при экстремальных значениях давления и температуры; новейшие данные 2019 г.

А. Гончаров

Ожидается, что водород проявляет замечательные свойства при экстремальных давлениях и температурах, обусловленных его низкой массой и, следовательно, склонностью к квантовым эффектам. Изучение таких явлений остается очень сложной задачей, несмотря на огромный технический прогресс, как в экспериментальных, так и в теоретических методах, с момента публикации последнего всестороннего обзора (McMahon *et al.*) в 2012 г. Для того чтобы охватить широкий диапазон давлений и температур, эксперименты по комбинационной и оптической спектроскопии, включая инфракрасную, были расширены. Новые методы импульсного лазерного нагрева и тороидальной алмазной наковальни вместе с защитными слоями значительно улучшили возможности статического сжатия. Были также проведены измерения электропроводности при гораздо больших значениях давления, чем предыдущие, и распространены на низкие температуры. Кроме того, методы динамического сжатия были значительно улучшены, больше ориентированы на изоэнтропическое сжатие, что дало возможность исследовать широкий спектр термодинамических состояний *P*–*T*. В последнее время с развитием новых экспериментальных инструментов и методов загрузки образцов ускорился поиск металлического водорода, что позволило получить множество рассмотренных в этой работе новых данных.

Ключевые слова: водород, экстремально высокие давления, твердая фаза водорода, плазменный переход, металлический водород.